Thermal Stability of O−H and O−Alkyl Bonds in *N*-Alkoxyamines. A Density Functional Theory Approach

P. Marsal,[†] M. Roche,[†] P. Tordo,[‡] and P. de Sainte Claire*,[†]

Laboratoire de Chimie Théorique, UMR 6517, CNRS et Universités d'Aix-Marseille I et III, Avenue Escadrille Normandie-Niemen, Case 521, Marseille, 13397 Cedex 20, France, and Laboratoire SREP, UMR 6517, CNRS et Universités d'Aix-Marseille I et III, Case 521, Avenue Escadrille Normandie-Niemen, Marseille, 13397 Cedex 20, France

Received: January 20, 1999

The O−C bond dissociation energy ($\Delta H_r^o(T)$) in alkoxyamines appears to play a key role in the nitroxide-mediated living free radical polymerizations, and an efficient control of the process can be achieved for $\Delta H_r^o(T)$ between 20 and 30 kcal/mol. We report in this paper density functional theory calculations of the O−H and O−C bond dissociation energies of different hydroxylamines and alkoxyamines. Optimization procedures, basis set effects, and exchange−correlation functionals are compared and tested against experimental data. Finally, the bond dissociation energy of (*N*-*tert*-butyl-1-diethylphosphono-2,2-dimethylpropylnitroxide)-R″ (where R″ = benzyl, styryl), is reported. This last result is especially important since SG1 is the most efficient to-date nitroxide radical in nitroxide-mediated polymerizations of styrene and acrylates.

Introduction

Nitroxide-mediated "living" free radical polymerization is a rapidly developing field which has opened up a new and potentially wide route to well-defined polymers, and as such, has driven both academic and industrial interests.[1−6] The control exerted by the nitroxide radical RR′NO· over the polydispersity of growing polymer chains depends on its ability to reversibly couple with polymeric radicals R″·:

$$\mathrm{RR'NO{-}R''} \underset{k_{-1}}{\overset{k_1}{\rightleftharpoons}} \mathrm{RR'NO\cdot} + \mathrm{R''\cdot} \qquad (1)$$

If k_1/k_{-1} is very small, polymeric radicals are scavenged by the nitroxide radical, and the polymerization process finishes. On the other hand, if k_1/k_{-1} gets too large, reaction 1 is not slow enough: *R″*· not only reacts with growing polymer chains but self-terminates as well, and the polymerization process is no longer controlled. Thus, a good control can be achieved for intermediate k_1/k_{-1} ratios. Experimentally, one seeks k_1/k_{-1} between 10^{-11} and 10^{-9} mol L^{-1}. Polymers that are produced in this way present low polydispersity indices and well-defined chain-end structures. Moreover, these polymers are more stable and present remarkable properties of mechanical stress. H. Fischer has pointed out that the kinetics of polymerizations involving nitroxide radicals are closely related to a general phenomenon which appears in reactions where transient and persistent (stable) radicals are formed simultaneously, the persistent radical effect.[7]

Assuming that both forward and backward reactions are single-step processes, the heat of reaction 1, $\Delta H_r^o(T)$, can be deduced from kinetic data and equation 2:

$$k_1/k_{-1} = (A_1/A_{-1}) \exp(-\Delta H_r^o(T)/RT) \qquad (2)$$

where A_1/A_{-1} is the ratio of the forward and backward reaction Arrhenius prefactors in equilibrium 1. It is commonly assumed that A_1/A_{-1} is constant for a range of reactions that involve similar species. Thus, the magnitude of $\Delta H_r^o(T)$ partially controls the polymerization process: if $\Delta H_r^o(T)$ is too large or too small, one does not get control over polydispersity indices. In practice, $\Delta H_r^o(T)$ values in the 20−30 kcal/mol range at room temperature are sought.

2,2,6,6-Tetramethyl-1-piperidinoxyl radical (Tempo·, see 4a) was first reported to have the ability to control the polymerization process,[1] but soon after, di-*tert*-butyl nitroxide radical (Dtbn·, see eq 4b) was shown to be even more effective (conversion rates were 3 times larger).[2,4,8] This field is currently undertaking a major development toward synthesis of better nitroxide radicals so that narrow polydispersity polymers and fast conversion rates could be obtained.

Heats of reaction for eqs 3, 4a, and 4b have been computed by semiempirical methods,[1,2,4,9,10] with the AM1 and PM3 Hamiltonians. In eqs 4a and 4b, R″ represents alkyl substituents. From now on, $\Delta H_r^o(T)$ will be indistinctly called "heat of reaction" or "bond dissociation energy" (BDE). The term "classical bond dissociation energy" (i.e., D_e) will be used to represent the difference in electronic energy between products and reactants, and will not include zero-point energy or enthalpic contributions (see the Method section).

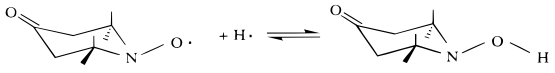

(3)

Tempo .

(4a)

Dtbn .

(4b)

ΔH_r^o(298 K) of 70.8 kcal/mol for reaction 3 was reported

* Author to whom correspondence should be addressed.

[†] Laboratoire de Chimie Théorique UMR 6517, CNRS et Universités d'Aix-Marseille I et III.

[‡] Laboratoire SREP, UMR 6517, CNRS et Universités d'Aux-Marseilles I et III.

10.1021/jp990202l CCC: $18.00
Published on Web 03/24/1999

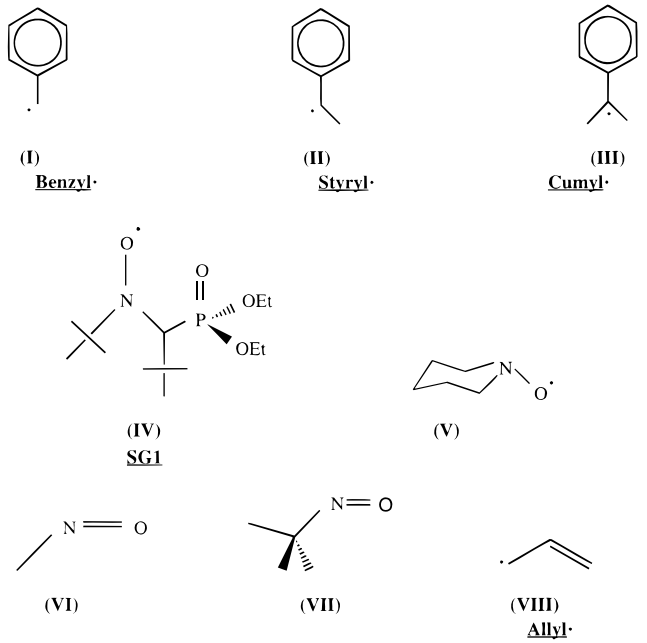

Figure 1. Chemical structures of selected molecules.

from AM1 theoretical calculations[9] in excellent agreement with experimental data ($\Delta H_r^{o,exp}(298\ K) = 71.9$ kcal/mol). In another study,[2] heats of reaction for eqs 4a and 4b and R″· = Styryl· (see **II** in Figure 1), were calculated with the AM1 and PM3 Hamiltonians: the Dtbn−Styryl BDE (17 kcal/mol with AM1) was reported to be smaller than that of Tempo−Styryl (22 kcal/mol with AM1). This is in agreement with experimental rates of polymer conversions: polymerization rates for styrene were shown to be faster with Dtbn· than Tempo·.[2] In this study, important differences (of the order of 5 kcal/mol) were reported between AM1 and PM3 bond dissociation energies.

A new nitroxide radical[11] [*N-tert*-butyl-1-diethylphosphono-2,2-dimethylpropylnitroxide (see **IV** in Figure 1), hereafter called SG1] was synthesized in our laboratory. Using SG1 to control the polymerization of styrene led to polydispersity indices between 1.1 and 1.3 and polymerization rates much faster than those obtained with Tempo·. Moreover, SG1 was even able to control the polymerization of acrylates, while Tempo· did not.[12] In an attempt to explain this difference of behavior, semi-empirical calculations were performed in our laboratory.[10] However, preliminary results did not agree with these experimental findings, and we decided to perform high-level ab initio calculations on similar systems. It was recently shown that density functional theory (DFT) methods gave quite accurate ESR hyperfine coupling constants (HFCCs) for nitroxide,[13] peroxyl,[14] and alkyl[15−17] radicals, while they presented the major advantage of being computationally cheaper than configuration interaction methods. Though literature is scarce about the computation of BDEs for homolytic dissociation processes with DFT methods, results are promising.[18−20] The O−H bond dissociation energy in phenol was calculated with the B3LYP method[18,19,21] and shown to agree within 5% (from the largest basis set calculation) of the experimental value. Similarly, the DFT method was shown to give accurate ionization potentials for conjugated alkyl radicals.[20]

In our work, we report theoretical DFT calculations of $\Delta H_r^o(T)$ for reactions 4a and 4b where R″· represents saturated and conjugated alkyl radicals. Results will be compared with experimental data when available.

Method

Thermodynamics. The following relationship holds between $\Delta H_r^o(T)$ and the classical electronic O−R″ bond dissociation energy, D_e:

$$\Delta H_r^o(T) = D_e + \Delta ZPE + \Delta H_{trans} + \Delta H_{rot} + \Delta H_{vib} - RT \quad (5)$$

where ΔZPE is the difference in zero-point energy between the alkoxyamine and the reactants. ΔH_{trans}, ΔH_{rot}, and ΔH_{vib} are the different contributions from translational, rotational, and vibrational degrees of freedom to the heat of reaction. Under equilibrium conditions, these can be obtained from statistical thermodynamics. In this respect, vibrational frequencies were computed at the Hartree−Fock level and scaled by 0.8929 to correct for known systematic errors.[22] It is the harmonic vibrational frequencies that were used in this work, and no attempt was made to correct the low vibrational modes by hindered rotor partition functions[23] since this would made a negligible difference in the calculation of the BDEs (less than 1%).

Electronic Structure Calculations. The DFT method was used to calculate D_e. In the DFT method, the energy is represented by a functional of the electron density ρ.[24] It is separated into different contributions, one of which being the exchange−correlation energy $E_{XC}[\rho]$, which arises from same spin and different spin interactions.

Exchange−correlation functionals used in this work always included gradient correction for both exchange and correlation functionals. Since many different expressions for $E_{XC}[\rho]$ are used in the literature, it was necessary to restrict the range of functionals that will be compared here. We decided on selecting the most widely used exchange−correlation functionals that went beyond the local density approximation. These include BLYP, a pure DFT functional where the nonlocal terms are represented by the LYP (Lee, Yang and Parr) functional,[25] as well as B3LYP,[25] B3P86,[26,27] and B3PW91,[28,29] three hybrid DFT functionals, i.e., a mixture of Hartree−Fock and DFT exchange,[30] with a DFT correlation term, the latter being different for the three methods. The P86 and PW91 are acronyms for the Perdew, and the Perdew and Wang correlation corrections, respectively.

Energies for the open-shell species were computed with spin-polarized hamiltonians. The effect of polarization, and diffuse and/or valence atomic orbitals in the basis set was also examined in this work. All ab initio computations were performed with the Gaussian94 suite of programs.[31] In the next sections, it will be shown that there is no need to go beyond the Hartree−Fock approximation to get accurate optimized geometries of all the species involved. This treatment is also justified since computation times would be scaled up by a factor of 4 or more, if better correlation treatments had been used.[32] Moreover, the very rapid expansion of the field, i.e., nitroxide-mediated living free radical polymerization, prompted us to develop a feasible and reliable method that could be used for larger polymeric species. Thus, it seemed important to address the drawbacks of such a method, if any, in detail.

Optimization Procedure: $H_2NO\cdot + H\cdot \rightleftharpoons H_2NO-H$. In this section, it will be shown that full optimization at the DFT level of theory is not necessary to properly describe the geometries of the involved species. The simplest nitroxide radical is $H_2NO\cdot$. Since $H_2NO\cdot$ is comprised of only two heavy atoms, a thorough optimization treatment can easily be performed for this species, and it will be presented here. Though

TABLE 1: Structural Parameters and Absolute Energies of the $H_2NO^{\bullet}$ and H_2NOH Species Optimized at Different Levels of Theory[a]

		B3P86/6-3 1G**// HF/6-31G**	B3P86/6-31G**
$H_2NO^{\bullet}$	NO	1.274	1.274
	NH	0.998	1.018
	HNO	116.1	119.1
	α[b]	32.4	20.5
	E (Hartrees)[c]	−131.3896542	−131.3909290
H_2NOH	NO	1.403	1.434
	NH	1.002	1.020
	HNO	105.1	103.8
	α[b]	67.0	64.2
	OH	0.943	0.964
	E(Hartrees)[c]	−132.0364526	−132.0380061
D_e (kcal/mol)[d]		81.6	81.7

[a] Distances in Å, angles in degrees. [b] α is the angle between the N−O bond and the plane formed by the H_2N subset of atoms (see Figure 2). [c] Electronic energy of the respective species. [d] Classical electronic O−H bond dissociation energy.

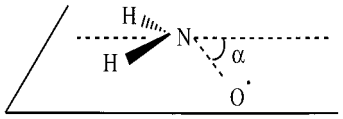

Figure 2. Definition of the α angle. Defined by the angle between the plane formed by the HNH subset of atoms and the NO bond.

much theoretical work has been dedicated to this species in the literature because of its small size,[33−37] it is not stable enough to be observed experimentally. Comparison between full geometry optimization at the DFT level with the B3P86 functional and the 6-31G** basis set (further shortened into B3P86/6-31G**) and a DFT single-point energy computation on a geometry optimized at the Hartree−Fock level with the 6-31G** basis set (further shortened into B3P86/6-31G**//HF/6-31G**) is presented in Table 1. Although bond distances are in very good agreement between the two methods (the difference is less than 3%), the NO bond in the closed shell species (H_2NO-H) was underestimated when optimization was performed at the Hartree−Fock level. This effect was also reported[38] in a comparative study of DFT and Hartree−Fock (HF) optimization procedures for piperidine-*N*-oxyl (see **V** in Figure 1): a 3% difference in the N−O bond length was observed between HF and the BLYP functional with the 6-31G* basis set. Similarly, Hartree−Fock treatments underestimated the N═O bond length by as much as 5% in nitrosomethane (see **VI** in Figure 1) and 2-methyl-2-nitrosopropane (see **VII** in Figure 1) molecules.[39]

Similarly, N−O bond lengths computed by Hartree−Fock methods were always smaller than experimental bond lengths for the alkoxyamines and nitroxide radicals described in our work.

It is also interesting to note that full DFT optimization favors larger variations of the α angle (see Figure 2 for a description of this angle and footnote *b* in Table 1) during the course of the reaction. This angle gives information about the planarity of the system and the hybridization at the nitrogen atom. Thus, optimizing at the Hartree−Fock level underestimates the change in hybridization during the reaction. In one study,[34] a CI calculation gives results for $H_2NO^{\bullet}$ in agreement with our findings. They report: N−O = 1.292 Å, N−H = 1.018 Å (see Table 1 for comparison). More recent work[36] reported restricted open-shell Hartree−Fock calculations for $H_2NO^{\bullet}$ and structural parameters (N−O = 1.273 Å, N−H = 1.005 Å, and HNH = 115.50°) that compared well with our unrestricted Hartree−Fock results in Table 1.

On the contrary, these studies report (α = 26.1°[34] and α = 36.5°,[36] respectively, whereas α = 20.5° in our work (full optimization procedure). However, such large variations of the α angle do not have much incidence on the energetics of $H_2NO^{\bullet}$ because the potential well about the minimum energy configuration for α deformations is very shallow and anharmonic.[34] The barrier for interconversion at the nitrogen center in $H_2NO^{\bullet}$ was reported to be of the order of 1 kcal/mol.[36,40] This interconversion barrier is expected to be much higher for Tempo• and Dtbn• because steric effects are more important there. Consequently, we expect much smaller variations of the α angle between different optimization treatments for Tempo• and Dtbn•. Similarly, α does not vary much between the Hartree−Fock and DFT optimization procedures for H_2NOH, in agreement with the preceding discussion: the interconversion barrier for H_2NOH at the nitrogen center is expected to be much higher than that for $H_2NO^{\bullet}$, and the potential well about the minimum energy structure much steeper.

It will be shown below (see the Results and Discussion section) that there is not much of a basis set effect on structural parameters. Although highly accurate structures could be obtained by a full optimization procedure, the stabilization energy for each species (less than 1 kcal/mol) is not sufficient enough to justify such a treatment. Moreover, D_e varies by less than 0.1 kcal/mol between the two treatments. In this work, species will be optimized at the Hartree−Fock level, and single-point energy calculations will be performed at the DFT level. Similar procedures are reported in the literature for homolytic dissociation reactions.[20,41]

Optimization Procedure: Tempo• + Cumyl• ⇌ Tempo−Cumyl. Since we decided to optimize the geometries at the Hartree−Fock level, it was necessary to address the question of a possible basis set effect. Results of geometry optimizations and experimental structures for Tempo• and Tempo−Cumyl (Cumyl• is represented by **III** in Figure 1) are presented in Table 2. Results for the Cumyl radical did not show significant change between basis sets, and as such, are not represented in Table 2. The Tempo−Cumyl system was chosen because it represents the largest species studied here.

Table 2 shows that there is no significant difference between results obtained with different basis sets, and it appears that a 6-31G* basis is sufficient to obtain converged geometries. Adding valence region functions on the N and O atoms resulted in shrinking the N−O bond by 0.006 Å. This effect was also observed by Barone et al. in nitronyl nitroxide radicals.[45] Good agreement is reached between theoretical and experimental values (see Table 2), and much of the eventual discrepancy (small N−O and O−C bonds) can be imputed to the optimization procedure (see discussion in the preceding section). There is good agreement between ab initio and experimental results for the α angle for both Tempo• and Tempo−Cumyl species. This was expected and discussed above. Comparison between experimental and theoretical results for the Tempo−Styryl (Styryl• is represented by **II** in Figure 1) are very similar to those presented in Table 2, and they are not shown here. Moreover, results for Dtbn• show even better agreement with experiment: N−O = 1.264 Å and 1.280 Å for theoretical and experimental results,[46] respectively. Last, we computed a significant difference of 3 kcal/mol for D_e between calculations with the 6-31G* and the 6-31G** basis sets (full DFT optimization procedure). This was expected since the latter includes polarization functions on hydrogen atoms. Thus, adequate basis sets will include polarization functions on both atoms that make the new bond. Consequently, in reactions 4a

TABLE 2: Optimized Geometries of Tempo−Cumyl Species at the Hartree−Fock Level and Different Basis Sets[a]

	expt[b]	6-31G*	6-31G+*	6-31G**	6-31G+**	6-311G+*(N,O)/6-3 1G+*[d]
			Tempo•			
NO	1.296	1.261	1.261	1.261	1.261	1.255
⟨NC⟩	1.482	1.484	1.486	1.484	1.486	1.486
⟨C−CH_3⟩	1.532	1.537	1.537	1.537	1.537	1.537
CNO	115.6	115.2	115.4	115.2	115.3	115.4
α[e]	19.4[c]	20.9	20.4	21.0	20.3	20.1
			Tempo−Cumyl			
NO	1.456	1.406	1.406	1.406	1.406	1.401
⟨NC⟩	1.501	1.492	1.493	1.493	1.494	1.493
⟨C−CH_3⟩	1.530	1.538	1.538	1.538	1.538	1.538
⟨CNO⟩	106.4	108.1	108.2	108.1	108.2	108.3
α[e]	56.0	52.7	52.6	52.7	52.6	52.2
OC	1.479	1.438	1.440	1.439	1.441	1.437
NOC	117.1	120.9	121.0	120.9	121.0	121.2

[a] Distances in Å, angles in degrees; < > means average. [b] Ref 42 for Tempo• and ref 43 for Tempo−Cumyl. [c] Ref 44. [d] Means that a 6-311G+* basis set was used on the nitrogen and oxygen atoms, whereas a 6-31G+* basis set was used for all other atoms. [e] α is the angle between the N−O bond and the plane formed by the CNC subset of atoms.

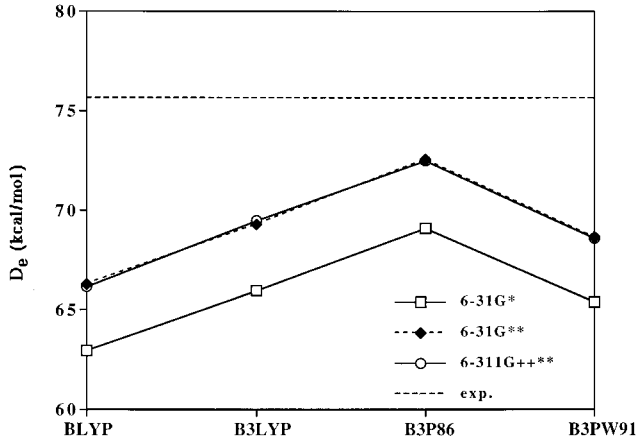

Figure 3. Tempo−H: classical bond dissociation energies (D_e, see text) in kcal/mol for selected DFT functionals and basis sets.

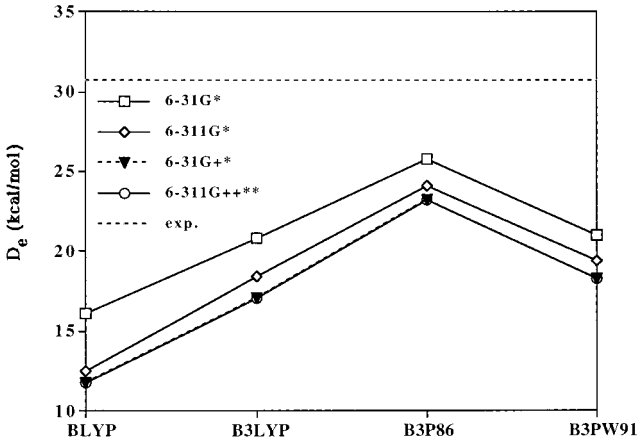

Figure 4. Tempo−Cumyl: classical bond dissociation energies (D_e, see text) in kcal/mol for selected DFT functionals and basis sets.

and 4b, geometries will be optimized at the Hartree−Fock level with the 6-31G* basis set for R″• = alkyl•, and the 6-31G** basis for R″• = H•.

However, although the choice of a basis set does not have much influence on geometric structures, one expects a much larger incidence on the energetics of the systems. In the next section, the importance of exchange−correlation functionals is examined.

Results and Discussion

Functionals. As stated earlier, four different functionals, i.e., a pure DFT (BLYP) and three hybrid functionals (B3LYP, B3P86, B3PW91), were examined in this work. The influence of the basis set on the classical bond dissociation energy of two model species (Tempo−H and Tempo−Cumyl) is also presented here.

Results are presented in Figures 3 and 4. The dashed line represents D_e^{exp}, the experimental classical bond dissociation energy for the system. It was deduced from the experimental heat of formation by removing enthalpic contributions computed at the Hartree−Fock level (see the Method section). The near constant energy difference between any two given basis sets and different exchange−correlation energy functionals is the most important result from these data: the different curves are simply shifted up or down from one another. Thus, it appears possible to separate the influence of the functional and the choice of a basis set.

Different exchange−correlation functionals are widely used in the literature, and it becomes exceedingly difficult to be able to predict the best $E_{XC}[\rho]$ for a given range of species. One way to address this question is to test different functionals for a given type of molecules against experimental data.[47]

Among the four correlation energy functionals used here, it is the Perdew functional (P86) that gives results in closest agreement with experiment. The LYP and the Perdew and Wang (PW91) functionals gave inferior results. Interestingly, the same conclusions were drawn in the work of Politzer et al.[48] where DFT ionization potentials of 12 small organic molecules were compared with experiment. Best results were obtained with the B3P86 method, whereas B3PW91, B3LYP, and BLYP functionals gave inferior results. It is also remarkable that, in their work, ionization potentials obtained from B3LYP and from B3PW91 differed by less than 0.1 kcal/mol. This effect is reported here as well: very similar values for D_e are obtained between the B3LYP and B3PW91 methods (see Figures 3 and 4).

The Perdew (P86) and the Perdew and Wang (PW91) correlation functionals differ by the real-space cut-off value of the gradient expansion approximation. In P86, this cut-off was chosen to reproduce the correlation energy of the neon atom, whereas it was set to satisfy the constraint for the correlation hole in PW91. Moreover, the LYP functional was calibrated on the helium atom, a species with zero parallel spin-correlation energy, whereas in neon, about 21% of the correlation energy

arises from parallel spin contributions.[49] This may explain the better B3P86 results for species that contain second-row elements.

B3LYP is much used in the literature to compute ESR hyperfine coupling constants (HFCCs) for organic radicals,[15−17] since it gives results that are in good agreement with experiment. Although the B3LYP method in conjunction with standard Gaussian basis sets gives satisfactory results, it was shown that the Perdew correlation functional gave accurate HFCCs for small organic radicals when large non-standard basis sets such as IGLO-III were used.[50] But most importantly, comparative studies between functionals for large molecules are very scarce. Such a study was performed by Wetmore et al.[14] in a DFT investigation of HFCCs in peroxyl radicals. Their work shows excellent agreement between experimental HFCCs and B3LYP data (an absolute mean deviation between calculated and experimental results on the terminal oxygen of 4.7 G was reported, i.e., a 20% discrepancy). The B3P86 and B3PW91 functionals gave inferior results: mean deviation was about 8.4 G for both functionals. This study led to the conclusion that the LYP functional gave a better description of core correlation than the Perdew functional, which was expected since LYP was calibrated on the helium atom, a first row element, whereas the Perdew functional was calibrated on the neon atom, a second row element.

Comparison of B3LYP and B3PW91 functionals for the ionization potentials of conjugated radicals[20] showed that best agreement with experiment was obtained with the B3P86 functional, in agreement with the results presented here. The Perdew functional was also selected over the LYP functional in a comparative study of DFT and high-level coupled-cluster (CCSD) calculations of the activation energy barriers for the cyclization of enediyne species.[51] Both studies show that core electrons are better described with the LYP functional, whereas proper description of valence electrons where parallel spin correlation is important might require the Perdew functional.

Basis Sets: Tempo· + ·H ⇌ Tempo−H. Figure 3 shows that it is necessary to add polarization functions on the hydrogen atom that is bonding to the nitroxide radical oxygen atom. This results in a gain in energy of about 3 kcal/mol. Moreover, adding diffuse functions (on both heavy and hydrogen atoms) and/or split-valence region functions did not improve the results. The limit of our largest basis set (6-311G++**) is reached with the 6-31G** basis set, for all DFT methods (see Figure 3).

Last, it is seen from Figure 3 that the B3LYP/6-31G**//HF/6-31G** method gives excellent agreement with experiment (within 4%), and is suitable for the computation of O−H bond dissociation energies in hydroxylamines.

At this point it was necessary to check whether the limit of large basis sets was obtained with the B3LYP/6-31G*//HF/6-31G* method for all saturated R″· alkyl radicals, and the Tempo−^{t}Bu BDE was computed with the 6-311G++** basis set, since this was the largest saturated R″· we encountered in this work. A B3P86/6-311G++**//HF/6-31G* calculation for Tempo−^{t}Bu gave D_e of 33.8 kcal/mol, whereas a B3P86/6-31G*//HF/6-31G* calculation yielded D_e of 36.9 kcal/mol, i.e., a 10% difference. These results confirmed that a converged classical bond dissociation energy is obtained with our method.

Basis Sets: Tempo· + ·Cumyl ⇌ Tempo−Cumyl. Results for the Tempo−Cumyl species are presented in Figure 4. Adding diffuse functions on heavy atoms and/or split-valence region functions decreases D_e by favoring stronger stabilization of the radical species with respect to the Tempo−Cumyl species. The stabilization of radical species upon addition of diffuse functions in the basis set is very general. The C−H classical bond dissociation energy in methane was computed at the B3P86/6-31G**//HF/6-31G** and B3P86/6-31G+**//HF/6-31G+** levels of theory: we found D_e =115.9 and 114.6 kcal/mol, respectively, in agreement with the above statement. The same effect was observed for the O−C classical BDE in H_2NO−allyl (allyl· is represented by **VIII** in Figure 1) with a 2 kcal/mol difference between the B3P86/6-31G* and the B3P86/6-31G+*//HF/6-31G* calculations. Similarly to the results presented in Figure 4, split-valence region functions contributed to decreasing the H_2NO−allyl classical BDE by 1.6 kcal/mol.

Finally, single-point DFT calculations with the 6-31G* and the 6-31G** basis sets differed by 0.2 kcal/mol only. This last result shows that polarization functions on hydrogen atoms are not important here. It is interesting to note that the limit of the largest basis set (6-311G++**) is already reached with the 6-31G+* basis set. This means that diffuse and polarization functions on hydrogen atoms have no effect here. Interestingly, adding split-valence region basis functions (6-311G*) has a significant effect on D_e, but this contribution is fully accounted for by the 6-31G+* basis set, as well. This is due to the fact that diffuse functions extend much further than split-valence region functions (and share the same general shape). As such, diffuse functions take into account electronic contributions from the valence regions.

Finally, although the 6-31G+* seems adequate for this type of calculation, we decided to use the 6-31G* basis set and to estimate the effect of a truncated basis set. This was done in order to shorten computation times. It is interesting to note that this effect (about 3 kcal/mol) is similar for species of identical size (i.e., Tempo−Cumyl and Tempo−^{t}Bu) no matter the presence of a conjugated π electron system.

In conclusion, we decided to use the B3P86/6-31G**//HF/6-31G** and the B3P86/6-31G*//HF/6-31G* methods for computing O−H hydroxylamine and O−C alkoxyamine BDEs, respectively. A basis set correction of 3 kcal/mol was estimated from the above results: in order to obtain the limit of the very large basis set, 3 kcal/mol should be removed from the 6-31G* BDE. This correction should decrease with the size of the molecules: for hydroxylamines, results should not be corrected.

TABLE 3: Comparison of DFT and experimental RR′NO−R″ Bond Dissociation Energies (kcal/mol) for Different Hydroxylamine and Alkoxyamine Species[a]

	Tempo·		Dtbn·		SG1	
R″·	$\Delta H_r^o(T)$[c]	expt[d]	$\Delta H_r^o(T)$[c]	expt[d]	$\Delta H_r^o(T)$[c]	expt[d]
H·	66.6 (72.6)	69.6[e]	65.7 (71.6)	68.2[e]		
methyl·	44.1 (49.6)	47.1[f]	42.3 (47.8)			
ethyl·	40.6 (45.4)		− (−)			
isopropyl·	40.4 (44.6)		37.6 (42.0)			
tert-butyl·	33.3 (36.9)		30.3 (34.0)			
benzyl·	29.0 (34.4)	34.7[g]	− (−)		− (32.3)	30.0[i]
styryl·	26.3 (31.2)	30.8[g]	22.2 (27.4)		− (28.7)	27.9[i]
cumyl·	21.3[b] (25.8)	26.2[h]	18.8 (23.6)			

[a] Experimental and calculated results are for a temperature of 298 K unless otherwise stated (see *b* below). [b] *T* was set to 358 K, the experimental temperature in ref 52. [c] Calculated heat of reaction: "—" means "was not calculated"; D_e (see text) appears in parentheses. [d] Experimental heat of reaction. [e] Ref 53. [f] Ref 54. [g] Fischer, H., personal communication. [h] Ref 52. [i] Fischer, H., Tordo, P., et al., to be published.

Results

Classical electronic BDEs (D_e) were computed and corrected for enthalpic effects (see the Method section above). $\Delta H_r^o(T)$ is reported in Table 3 for reactions 4a and 4b, and different R″·. Results for hydroxylamines and small alkoxyamines are

in excellent agreement with experimental data. For the largest alkoxyamines, a basis set correction of 3 kcal/mol should be substracted from the 6-31G* results in Table 3: when this correction is included, bond dissociation energies for the sterically crowded Tempo−Benzyl, Tempo−Styryl, and Tempo−Cumyl molecules are 7−8 kcal/mol below the experimental BDEs. Steric effects are very important for these molecules: however, the B3P86/6-31G*//HF/6-31G* method, as already pointed out, fails to give accurate N−O and C−O bond lengths.[55] Therefore, optimizing at the DFT level would result in larger N−O and C−O bonds and thus, in larger calculated BDEs.

However, the relative order of the BDEs in Table 3 for a given nitroxide radical and different R″ follows the very general rule that the larger the alkoxyamine, the smaller the BDE. In Table 3, $\Delta H_r^o(T)$ continuously decreases in a column: this strongly supports the dependence of $\Delta H_r^o(T)$ on the size of R″·, and the importance of steric effects. The hyperconjugation of R″· is not important here.

Second, in this series of R″· radicals, only Styryl· and Cumyl· can undergo polymerization, whereas all the others cannot. We already saw that, in practice, $\Delta H_r^o(T)$ in the 20−30 kcal/mol range is expected to achieve efficient initiation and control of the polymerization process: only Styryl· and Cumyl· satisfy this requirement (see Table 3), in agreement with experimental findings. However, $\Delta H_r^o(T)$ may not be the only important parameter in order to achieve an efficient polymerization control: in fact, the assumption of constant A_1/A_{-1} ratio in eq 2 may be seriously questioned if solvent effects are important for equilibrium (eq 1). The experimental measurements for Tempo−Cumyl were made in *tert*-butylbenzene,[52] which favors "dipole/induced dipole" long-range interactions. Indeed, there is strong evidence that nitroxides are strongly solvated in polar and polarizable solvents by stabilization of the dipolar form B in eq 6 below:[56]

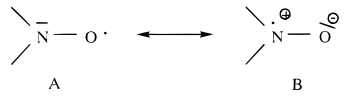

(6)

The source of the discrepancy between calculated and experimental results in Table 3 for Tempo−Cumyl may find an explanation here.

Finally, the B3P86/6-31G*//HF/6-31G* method was used to compute the SG1−Benzyl and SG1−Styryl classical BDEs (SG1 is represented by **IV** in Figure 1). We found D_e(SG1−Benzyl) = 32.3 kcal/mol and D_e(SG1−Styryl) = 28.7 kcal/mol. $\Delta H_r^o(T)$ of 24 and 21 kcal/mol can be estimated from these values, respectively, by removing basis set (3 kcal/mol) and enthalpic (5 kcal/mol) effects. Experimental values of 30.0 and 27.7 kcal/mol, respectively, at 298 K,[57] compare well with our calculated results. Moreover, the SG1−Styryl species enhances polymerization rates with respect to those with Tempo−Styryl, suggesting that ΔH_r^o(SG1−Styryl) might be lower than ΔH_r^o(Tempo−Styryl).[12] We report results in this work that clearly corroborate this experimental observation.

Conclusions

Alkoxyamines play a key role in the nitroxide-mediated living polymerizations and most experimental findings emphasize the importance of the alkoxyamine O−C bond dissociation energy for these processes. In this paper we reported DFT calculations of $\Delta H_r^o(T)$ for reaction 1. In reaction 1, RR′NO−R″ were different alkoxyamine species, some of which are used in the industry. Excellent agreement with experiment was reached for the smallest hydroxylamines and alkoxyamines at the B3P86/6-31G**//HF/6-31G** and B3P86/6-31G*//HF/6-31G* levels of calculation, respectively. We showed that diffuse functions on heavy atoms are needed for a proper description of the more sterically crowded species. Basis set superposition errors (BSSE) are expected to be negligible for the results obtained with the largest basis set (6-311G++**) and were not included here. Experimental trends were very well reproduced by our results, whether the nitroxide radical was Tempo· or SG1.

We are now developing our efforts toward two directions: first it is important to test whether solvent effects have an incidence on D_e and the geometries of the species. This will be further investigated by ab initio and molecular dynamics methods. Second, the hypothesis of a single-step process for equilibrium (eq 1) is questionable: reaction path calculations are under way in our laboratory toward a better understanding of alkoxyamine homolytic dissociations.

Acknowledgment. The authors thank Dr. C. Jablon (Elf-Aquitaine) and Dr. J. F. Pierson (Elf-Atochem) for their interest and financial support.

References and Notes

(1) Georges, M. K.; Veregin, R. P. N.; Kazmaier, P. M.; Hamer, G. K. *Trends Polym. Sci.* **1994**, *2*, 66.
(2) Kazmaier, P. M.; Moffat, K. A.; Georges, M. K.; Veregin, R. P. N.; Hamer, G. K. *Macromolecules* **1995**, *28*, 1841.
(3) Puts, R. D.; Sogah, D. Y. *Macromolecules* **1996**, *29*, 3323.
(4) Moad, G.; Rizzardo, E. *Macromolecules* **1995**, *28*, 8722.
(5) Hawker, C. J. *Acc. Chem. Res.* **1997**, *30*, 373.
(6) Fukuda, T.; Terauchi, T. *Chem. Lett.* **1996**, 293.
(7) Fischer, H. *Macromolecules* **1997**, *30*, *5666.*
(8) Rizzardo, E. *Chem. Aust.* **1987**, *54*, 32.
(9) Cogen, J. M. *Polym. Degrad. Stab.* **1994**, *44*, 49.
(10) Gaudel, A.; Tordo, P.; Siri, D. To be published.
(11) Grimaldi, S.; Le Moigne, F.; Finet, J. P.; Tordo, P.; Nicol, P.; Plechot, M. *International Patent*, WO 96124620, August 15, 1996.
(12) Benoit, D.; Grimaldi, S.; Finet, J.-P.; Tordo, P.; Fontanille, M.; Gnanou, Y. *Controlled Radical Polymerization,* Chapter 14; Matyjaszewski, K., Ed.; ACS Publications Division and Oxford University Press, **1998**, *685*, 225.
(13) Zheludev, A.; Barone, V.; Bonnet, M.; Delley, B.; Grand, A.; Ressouche, E.; Rey, P.; Subra, R.; Schweizer, J. *J. Am. Chem. Soc.* **1994**, *116*, 2019.
(14) Wetmore, S. D.; Boyd, R. J.; Eriksson, L. A. *J. Chem. Phys.* **1997**, *106*, 7738.
(15) Batra, R.; Giese, B.; Spichty, M.; Geischeidt, G.; Houk, K. N. *J. Phys. Chem.* **1996**, *100*, 18371.
(16) Rega, N.; Cossi, M.; Barone, V. *J. Chem. Phys.* **1996**, *105*, 11060.
(17) Zuilhof, H.; Dinnocenzo, J. P.; Reddy, A. C.; Shaik, S. *J. Phys. Chem.* **1996**, *100*, 15774.
(18) Wright, J. S.; Carpenter, D. J.; McKay, D. J.; Ingold, K. U. *J. Am. Chem. Soc.* **1997**, *119*, 4245.
(19) Brinck, T.; Haeberlein, M.; Jonsson, M. *J. Am. Chem. Soc.* **1997**, *119*, 4239.
(20) Jursic, B. S. *Int. J. Quantum Chem.* **1997**, *62*, 291; Jursic, B. S. *J. Chem. Soc., Perkin Trans. 2* **1995**, 700.
(21) Wu, Y.-D.; Lai, D. K. W. *J. Org. Chem.* **1996**, *61*, 7904.
(22) Pople, J. A.; Scott, A. P.; Wong, M. W.; Radom, L. *Isr. J. Chem.* **1993**, *33*, 345.
(23) Truhlar, D. G. *J. Comput. Chem.* **1991**, *12*, 266.
(24) Hohenberg, P.; Kohn, W. *Phys. Rev.* **1964**, *136*, B864.
(25) Lee, C.; Yang, W.; Parr, R. G. *Phys. Rev. B* **1988**, *37*, 785.
(26) Perdew, J. P. *Phys. Rev. B* **1986**, *33*, 8822.
(27) Perdew, J. P. *Phys. Rev. B* **1986**, *34*, 7406.
(28) Perdew, J. P.; Wang, Y. *Phys. Rev. B* **1992**, *45*, 13244.
(29) Perdew, J. P.; Chevary, J. A.; Vosko, S. H.; Jackson, K. A.; Pederson, M. R.; Singh, D. J.; Fiolhais, C. *Phys. Rev. B* **1992**, *46*, 6679.
(30) Becke, A. D. *J. Chem. Phys.* **1993**, *98*, 5648.
(31) Frisch, M. J.; Trucks, G. W.; Schlegel, H. B.; Gill, P. M. W.; Johnson, B. G.; Robb, M. A.; Cheeseman, J. R.; Keith, T.; Petersson, G. A.; Montgomery, J. A.; Raghavachari, K.; Al-Laham, M. A.; Zakrzewski, V. G.; Ortiz, J. V.; Foresman, J. B.; Cioslowski, J.; Stefanov, B. B.; Nanayakkara, A.; Challacombe, M.; Peng, C. Y.; Ayala, P. Y.; Chen, W.; Wong, M. W.; Andres, J. L.; Replogle, E. S.; Gomperts, R.; Martin, R. L.;

Fox, D. J.; Binkley, J. S.; Defrees, D. J.; Baker, J.; Stewart, J. P.; Head-Gordon, M.; Gonzalez, C.; Pople, J. A. *Gaussian94*, Revision E.2, Gaussian, Inc.: Pittsburgh, **1995**.

(32) Lozynski, M.; Rusinska-Roszak, D.; Mack, H.-G. *J. Phys. Chem. A* **1998**, *102*, 2899.

(33) Ellinger, Y.; Subra, R.; Rassat, A.; Douady, J.; Berthier, G. *J. Am. Chem. Soc.* 1975, *97*, 476.; Briere, R.; Claxton, T. A.; Ellinger, Y.; Rey, P.; Laugier, J. *J. Am. Chem. Soc.* **1982**, *104*, 34.

(34) Pauzat, F.; Gritli, H.; Ellinger, Y.; Subra, R. *J. Phys. Chem.* **1984**, *88*, 4581.

(35) Ricca, A.; Tronchet, J. M. J.; Weber, J.; Ellinger, Y. *J. Phys. Chem.* **1992**, *96*, 10779.

(36) Takase, H.; Kikuchi, O. *J. Phys. Chem.* **1994**, *98*, 5160.

(37) Komaromi, I.; Tronchet, J. M. J. *Chem. Phys. Lett.* **1993**, *215*, 444.

(38) Komaromi, I.; Tronchet, J. M. J. *J. Phys. Chem.* **1995**, *99*, 10213.

(39) Bentley, J.; Madden, K. P. *J. Am. Chem. Soc.* **1994**, *116*, 11397.

(40) Davis, T. D.; Christoffersen, R. E.; Maggiora, G. M. *J. Am. Chem. Soc.* **1975**, *97*, 1347.

(41) Boyd, S. L.; Boyd, R. J. *J. Phys. Chem.* **1994**, *98*, 11705.

(42) Bordeaux, D.; Lajzerowicz-Bonneteau, J.; Brière, R.; Lemaire, H.; Rassat, A. *Org. Magn. Reson.* **1973**, *5*, 47.

(43) Lemercier, C.; Henriet, C.; Tordo, P. *X-ray crystallographic data*, to be published.

(44) Rassat, A.; Rey, P. *Tetrahedron* **1973**, *29*, 1599.

(45) Barone, V.; Grand. A.; Luneau, D.; Rey, P.; Minichino, C.; Subra, R. *New J. Chem.* **1993**, 17.

(46) Andersen, B.; Andersen, P. *Acta Chem. Scand.* **1966**, *20*, 2728.

(47) Levine, I. N. *Quantum Chemistry*, 4th ed.; Prentice-Hall: Engelwood Cliffs, NJ, **1991**; Chapter 15.

(48) Politzer, P.; Abu-Ahwad, F. *Theor. Chem. Acc.* **1998**, *99*, 83.

(49) Becke, A. D. *J. Chem. Phys.* **1996**, *104*, 1041.

(50) Engels, B.; Eriksson, L. A.; Lunell, S. *Adv. Quantum Chem.* **1996**, *27*, 297.

(51) Chen, W.-C.; Chang, N.-Y.; Yu, C.-H. *J. Phys. Chem. A* **1998**, *102*, 2584.

(52) Kothe, T.; Marque, S.; Rainer, M.; Popov, M.; Fischer, H. *J. Chem. Soc., Perkin Trans. 2*, submitted.

(53) Mahoney, L. R.; Mendenhall, G. D.; Ingold, K. U. *J. Am. Chem. Soc.* **1973**, *95*, 8610; Bordwell, F. G.; Liu, W.-Z. *J. Am. Chem. Soc.* **1996**, *118*, 10819.

(54) Ciriano, M. V.; van Scheppingen, W. B.; Korth, H.-G.; Mulder, P. Private communication.

(55) N−O and C−O bond lengths calculated at the B3P86/6-31G*//HF/6-31G* level for Tempo−Cumyl were 1.406 and 1.438 Å, respectively (see Table 2), while the experimental bond lengths (X-ray structure) were 1.456 and 1.479 Å, respectively.[43]

(56) Beckwith, A. L. J.; Bowry, V. W.; Ingold, K. U. *J. Am. Chem. Soc.* **1992**, *114*, 4983.

(57) Fischer, H. Private communication.